European Journal of Orthopaedic Surgery & Traumatology (2019) 29:1399–1404
https://doi.org/10.1007/s00590-019-02463-x

ORIGINAL ARTICLE • SHOULDER - ARTHROPLASTY

Quantitative in vivo assessment of bone allograft viability using ^{18}F-fluoride PET/CT after glenoid augmentation in reverse shoulder arthroplasty: a pilot study

Josef Hochreiter[1] · Georg Mattiassich[1] · Wolfgang Hitzl[2] · Georg Weber[1] · Mohsen Beheshti[3] · Reinhold Ortmaier[1,4]

Received: 2 March 2019 / Accepted: 3 June 2019 / Published online: 6 June 2019

Abstract

Background Success after glenoid bone augmentation in total shoulder arthroplasty depends on osseous integration and non-resorption. Standard imaging techniques, such as computed tomography (CT) and X-rays, cannot quantify bone viability. Therefore, we introduce a new technique to assess graft viability using ^{18}F-sodium fluoride (^{18}F-NaF) PET–CT for femoral allografts in reverse total shoulder arthroplasty (RSA).

Materials and methods Patient charts were reviewed following glenoid augmentation using femoral allografts in reverse total shoulder arthroplasty. A total of seven patients were included in this study. ^{18}F-NaF PET–CT was used to assess graft viability and graft fusion. Semiquantitative assessment of ^{18}F-NaF uptake was performed by means of a standardized uptake value (SUV). Radiographs were used to assess fusion. The mean age of the patients at the time of follow-up was 83.4 years (range 79–92), and the mean follow-up was 44.4 months.

Results Viability and fusion were confirmed in all allografts using semiquantitative analysis of ^{18}F-NaF PET–CT by means of standardized uptake value (SUVmax). Metabolic activity of medullary region of a vertebral spine was defined as a reference background. The mean value of maximum tracer activity in the allograft was not statistically different from native bone in the reference vertebrae ($p = 0.14$).

Conclusions ^{18}F-NaF PET–CT is a practicable tool to quantitatively assess viability in large bone allografts after glenoid augmentation in RSA. The study shows viability and fusion in all allografts.

Level of Evidence Level IV, treatment study.

Keywords Bone allograft · Reverse shoulder arthroplasty · Viability · Fusion · PET-CT

✉ Reinhold Ortmaier
r.ortmaier@gmail.com

Josef Hochreiter
Josef.Hochreiter@ordensklinikum.at

Georg Mattiassich
georg.mattiassich@gmx.at

Wolfgang Hitzl
wolfgang.hitzl@pmu.ac.at

Georg Weber
georg.weber@bhs.at

Mohsen Beheshti
mohsen.beheshti@ordensklinikum.at

[1] Department of Orthopaedic Surgery, Ordensklinikum Barmherzige Schwestern Linz, Vinzenzgruppe Center of Orthopedic Excellence, Teaching Hospital of the Paracelsus Medical University Salzburg, Seilerstätte 4, 4020 Linz, Austria

[2] Department of Biostatistics, Paracelsus Medical University, Müllner Hauptstraße 48, 5020 Salzburg, Austria

[3] Department of Nuclear Medicine, Ordensklinikum Barmherzige Schwestern Linz, Vinzenzgruppe, Seilerstätte 4, 4020 Linz, Austria

[4] Research Unit for Orthopedic Sports Medicine and Injury Prevention, ISAG/UMIT, Eduard-Wallnöfer-Zentrum 1, 6060 Hall in Tirol, Austria

Introduction

Glenoid bone loss in shoulder arthroplasty (SA) is challenging for the orthopedic surgeon. To avoid eccentric loading and early glenoid loosening, it is crucial in reverse total shoulder arthroplasty (RSA) to implant the glenoid component in an anatomical position [1, 2]. Therefore, central or peripheral bone defects that alter version and joint line have to be corrected. In mild peripheral defects, eccentric reaming is recommended to correct version [3]. However, this procedure is limited to approximately 10° of retroversion [3]. In larger defects, bone grafts or augmented glenoid components are used [4, 5]. Although bone grafting is an established method to treat glenoid bone defects in SA, the results after autograft or allograft are heterogeneous [6–9]. An autograft can be harvested from the humeral head in primary cases or from the iliac crest in both primary and revision cases. Donor site morbidity and limited bone availability, which are the main limitations for autografts, remain matters of debate. Benefits of allografts include the lack of donor site morbidity and the large and quick availability of bone.

However, concerns about graft incorporation, resorption and viability of the graft may discourage surgeons to use allografts [4, 6, 9, 10].

A prerequisite for successful glenoid component fixation in SA and bone grafting is fusion and non-resorption of the graft. Therefore, graft viability is necessary to keep the bone and achieve glenoid ingrowth. Techniques for quantification of graft resorption and ingrowth include standard X-rays and computed tomography (CT) scans [7, 11]. However, radiographs and CT have shown to provide nearly equal fusion assessment accuracy and both techniques seem to overestimate fusion rates [12, 13]. Additionally, assessment of viability and metabolic processes in bone cannot be displayed and quantified using X-rays or standard CT. Molecular imaging techniques, such as hybrid positron emission tomography-computed tomography (PET–CT) by ^{18}F-sodium fluoride (^{18}F-NaF), have already been established for assessment of metabolic processes in the skeleton. It showed a promising role for the depiction of benign and malignant bone disorders as well as early assessment of bone remodeling process.

Although ^{18}F-NaF PET–CT has mainly been investigated in the field of oncology, it has also been described as a proper method to assess osseous integration and viability of bone allografts after large segmental reconstruction following en bloc spondylectomy [14].

The aim of this pilot study was to introduce this new technique for the assessment of bone viability and graft fusion using ^{18}F-NaF PET–CT after glenoid reconstruction using femoral allografts in RSA. We hypothesized that the enrichment pattern of the allograft is significantly different to native bone.

Materials and methods

Patients

For this retrospective study, we reviewed patient charts at our institution to evaluate all patients who underwent glenoid bone augmentation using a femoral allograft in RSA (Fig. 1). In the study period from 2006 to 2014, we found ten patients who fit this description. Of these ten patients, two patients died and one patient denied participating PET–CT examination, leaving seven patients in the study (six women and one man). The mean age of the patients at the time of follow-up was 83.4 years (range 79–92). The mean follow-up was 44.4 months (range 24–63). The dominant shoulder was affected in six patients. The right shoulder was affected in six patients and the left was affected in one patient. After a minimum follow-up period of 2 years, ^{18}F-NaF PET–CT was performed to assess viability and fusion of the femoral allograft. Additionally, standard X-rays were used to assess fusion. In standard X-rays, fusion was quantified as a percent of the medial side of the graft that was not fused to the glenoid side according to the technique described by Iannoti

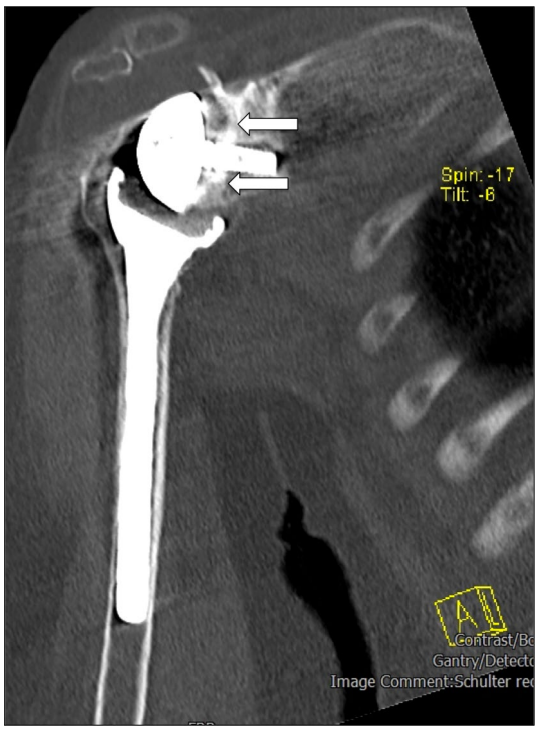

Fig. 1 RSA at final follow-up after 36 months. White arrows indicate medial border of the bone allograft. The allograft is incorporated without any signs resorption

and Frangiamore [11]. Fusion and viability were assessed by an experienced nuclear medicine board-certified nuclear medicine physician together with an orthopedic surgeon. This research has been approved by the IRB of the authors' affiliated institutions.

PET–CT scanning

The study was performed with a dedicated PET–CT scanner (GE Healthcare, Discovery 710) with an extended field-of-view full-ring high-resolution LSO PET component and a 128-slice spiral CT. The PET–CT system consisted of a full-ring PET scanner with a 15.7-cm transverse field of view, an in-plane resolution of 3.75 mm full width at half maximum at the center of the field of view. All PET scans were acquired in 3D time of flight mode (5-min emission per bed position), reconstructed with a standard iterative reconstruction ordered-subset expectation maximization (OSEM) iterative algorithm and reformatted into transverse, coronal and sagittal views. Acquisition started 60 min post-intravenous injection of ^{18}F-NaF (150 MBq) from in the shoulder (two beds position).

NaF binds to the sites of new bone formation and serves as a marker of bone blood flow and osteoblastic activity [15].

Two-third of bone is composed of minerals and one-third of collagen, extracellular matrix and a variety of bone lining cells. The mineral matrix is composed of calcium hydroxyapatite. The mechanism of uptake is similar for ^{18}F-NaF and technetium-99 m (99mTc) bisphosphonates. Following chemisorption of fluoride ions onto the surface of hydroxyapatite, they exchange with the hydroxyl (OH^-) ions in the crystal, forming fluorapatite. [16]

$$Ca_5(PO_4)_3OH + F \rightarrow Ca_5(PO_4)_3F + OH^-$$

CT data were captured with a high-beam current (120–330 mA) to acquire optimal image quality. The images were also reconstructed with a specific bone algorithm provided by the manufacturer and an ultra-high-resolution slice thickness of 0.6 mm. The reformatted, transverse, coronal and sagittal views were used for interpretation.

Semiquantitative analysis

Semiquantitative assessment of ^{18}F-NaF uptake was performed by means of a standardized uptake value (SUV).

SUVs were obtained by manually placing a volume of interest (VOI, 50% threshold) over the bone allograft on the shoulder that had been identified on visual analysis of static emission images between the central peg and the inferior locking screw of the baseplate (Fig. 2). By using attenuation-corrected PET data, SUVs were calculated as the ratio of regional radioactivity concentration (Becquerel/milliliter) divided by the injected amount of radioactivity (Becquerel) normalized to body weight in grams. Both maximum SUV (SUVmax) and mean SUV (SUVmean) were measured. However, to minimize partial volume effects, SUVmax within the VOIs rather than volumetric mean SUV was used for statistical analysis. In addition, a standard VOI was drawn over the medullary region of a vertebral spine as a

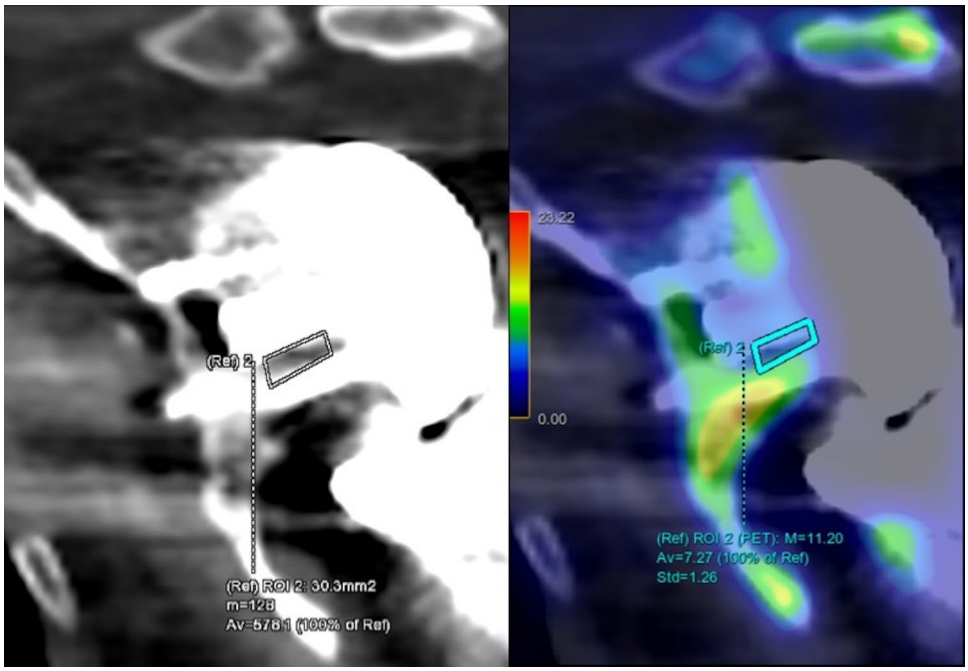

Fig. 2 ^{18}F-NaF PET/CT: coronal CT (left) and fusion PET/CT (right) view from the shoulder. VOI is manually drawn over the allograft for viability assessment. The localization and size of VOI were defined based on the corresponding transaxial and sagittal CT images

reference background VOI, and the SUVmax was measured to define the normal background SUV in the skeleton (Fig. 3).

Statistical methods

Data consistency was checked, and data were screened for outliers and normality using quantile plots. Independent Student's *t* tests and Whisker plots with 95% confidence intervals were used to illustrate the results. All reported tests were two-sided, and p values < 0.05 were considered statistically significant. All statistical analyses in this report were performed using Statistica 13 (Hill T. and Lewicki P. Statistics: Methods and Applications. StatSoft, Tulsa, OK).

Results

In the semiquantitative analysis, the mean value of SUVmax was 7.1 ± 1 within the allografts and 6.1 ± 1.1 in the reference vertebrae ($p = 0.14$, Fig. 4). Therefore, the enrichment pattern showed that viability in the allograft was not statistically different from the native reference vertebrae.

In all cases, fusion was confirmed in all allografts with ^{18}F-NaF PET–CT and X-rays (100% fusion).

Discussion

The main finding of this study was that metabolic activity of the allografts presenting the molecular bone remodeling and viability was comparable to normal medullary bone tissue on the reference vertebrae and fusion was achieved in all cases. Of course, this study has several limitations, the small sample size and retrospective design being the main ones. To enhance statistical power, larger series must be investigated to draw better conclusions regarding bone viability after large allograft augmentation in SA.

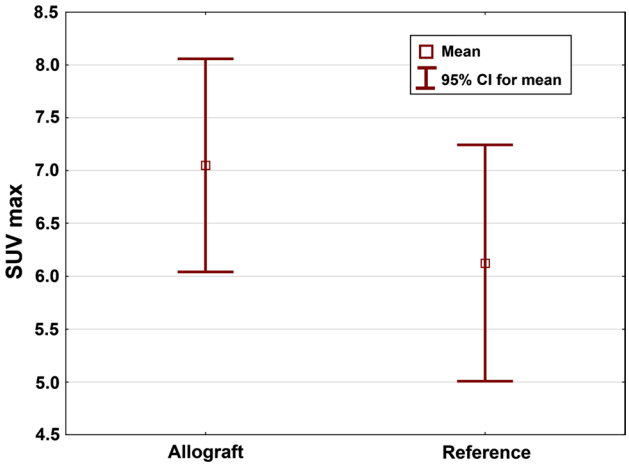

Fig. 4 Maximum standardized uptake value (SUV) is illustrated for allografts and for reference vertebrae

Feasibility of ^{18}F-NaF PET/CT in clinical practice

There is no major concern regarding the toxicity of this novel modality.

Furthermore, when comparing with 99Tc-labeled conventional bone scintigraphy, ^{18}F-NaF PET/CT has some advantages such as less plasma protein binding with resultant higher ability of the depiction of bone remodeling and faster serum clearance as well as shorter uptake time (30–45 min instead of 2–3 h), greater spatial resolution (2–4 mm instead of 10–15 mm), higher sensitivity and better image quality with higher target-to-background ratio [17]. Thus, it is more feasible and practicable in the routine clinical practice with ability to depict the early bone remodeling at molecular level [18].

Additionally, semiquantitative analysis is one of the additional advantages of ^{18}F-NaF PET/CT, which is not easily applicable on conventional imaging modalities. This feature allows reliable comparison of the metabolic activity in the

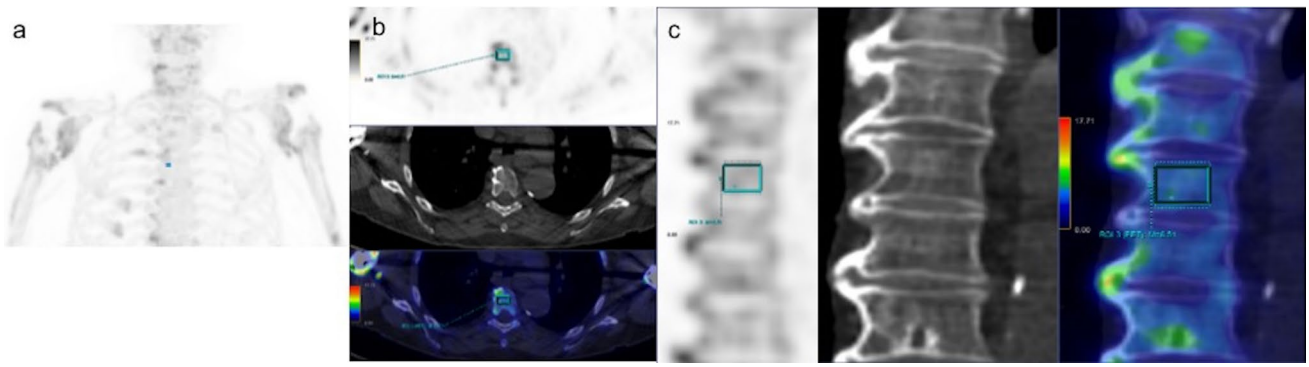

Fig. 3 ^{18}F-NaF PET/CT: **a** maximum intensity projection (MIP) PET image from thorax. **b** Transaxial ^{18}F-NaF PET/CT: PET (left), CT (mid) and fusion PET/CT (right). **c** Sagittal ^{18}F-NaF PET/CT: PET (upper), CT (mid) and fusion PET/CT (lower)

allografts with normal bone tissues for the assessment of viability.

However, metallic implants, such as shoulder prosthetics, may cause a limitation and result in high CT (or Hounsfield) numbers and generate streaking artifacts on CT images because of their high photon absorption. This increase in CT numbers results in correspondingly high PET attenuation coefficients, which leads to overestimation of the PET activity in that region and thereby to a false positive. Non-attenuated PET images, which do not manifest this error, can be used for visual assessment and to rule out metal-induced artifacts. However, performing semiquantitative analysis is not possible on non-corrected images. In recent years, different metal artifact reduction (MAR) methods have been developed for CT; however, these methods have not been implemented in PET/CT. MAR could be beneficial for the interpretation and quantification of PET/CT scans. Another approach is to correct SUV values with a coefficient factor depending on the type of prosthesis. Although all PET images were additionally assessed in non-corrected mode to rule out metal-induced artifacts in this study, the quantitative results may have been affected by metal-induced artifacts. Nevertheless, the objective of this pilot study was to introduce this novel molecular imaging approach for assessing bone allografts. Future studies are mandatory to proof validity of this technique before routine clinical application.

Allografts

Autologous bone grafting has drawbacks due to donor site morbidity, limited donor sites, differing bone sizes, shape of the graft configuration and limited bone availability.

Therefore, allografts seem to be a viable alternative due to their lack of donor site morbidity and the quick availability of large amounts of bone.

On the other hand, cryopreserved allografts are known to have no remaining vascularity, which is associated with high complication rates such as infection, fracture and nonunion. In a postmortem study by Enneking, the authors found limited bone remodeling and revascularization over time. In another study, the authors found incomplete ingrowth of cryopreserved allografts in histological studies [19, 20].

However, in this study we show metabolic processes in all allografts, demonstrating an enrichment pattern that is not significantly different from normal medullary bone activity on reference vertebrae.

In our institution, bone bank allografts are not irradiated. This may have contributed to the increased viability in our series. In all patients, a femoral allograft from the institution's bone bank was used. All allografts were harvested during total hip arthroplasty and were immediately frozen at − 70 °C without irradiation. Nevertheless, more patients need to be investigated to draw conclusions with regard to bone viability.

Results in the literature after allograft augmentation are heterogeneous [7, 9, 11, 21]. However, the results after RSA seem more promising than after hemiarthroplasty or anatomical total shoulder arthroplasty. The main reason is that the graft needs a metallic baseplate to support the native glenoid bone stock.

In a study by Iannotti and Frangiamore [11], the authors investigated 19 patients after large structural femoral allografts for glenoid reconstruction for shoulder hemiarthroplasty. Six of 19 patients showed more than 50% graft resorption, and four of those six exhibited less than 50% graft incorporation. In 13 patients, 100% graft incorporation was found after a minimum follow-up of 2 years.

In a study by Bateman and Donald [10], positive results were achieved after glenoid augmentation using a combined allograft–autograft construct. None of their patients showed loosening or implant failure after a follow-up of up to 36 months.

Jones et al. [6] followed reverse shoulder arthroplasties after glenoid augmentation using an autograft or allograft and found no difference in the clinical or radiological outcomes between the two graft types. Ultimately, 81% of all grafts fused with the native glenoid. The authors concluded that allografts seem to show equal results compared to autografts.

Conclusions

To conclude, ^{18}F-NaF PET–CT is a practicable tool to quantitatively assess viability in large bone allografts after glenoid augmentation in RSA. The study shows viability and fusion in all allografts.

Acknowledgements The authors, their immediate families and any research foundations with which they are affiliated have not received any financial payments or other benefits from any commercial entity related to the subject of this article.

Compliance with ethical standards

Conflict of interest The authors declare that they have no conflict of interest.

Ethical approval Ethical approval was obtained from Gemeinsame Ethikkommission der Barmherzigen Schwestern und Barmherzigen Brüder, study number: EKS 11/17.

References

1. Boileau P, Avidor C, Krishnan SG, Walch G, Kempf J-F, Molé D (2002) Cemented polyethylene versus uncemented metal-backed

glenoid components in total shoulder arthroplasty: a prospective, double-blind, randomized study. J Shoulder Elb Surg 11:351–359. https://doi.org/10.1067/mse.2002.125807
2. Fox TJ, Cil A, Sperling JW, Sanchez-Sotelo J, Schleck CD, Cofield RH (2009) Survival of the glenoid component in shoulder arthroplasty. J Shoulder Elb Surg 18:859–863. https://doi.org/10.1016/j.jse.2008.11.020
3. Nowak DD, Bahu MJ, Gardner TR, Dyrszka MD, Levine WN, Bigliani LU, Ahmad CS (2009) Simulation of surgical glenoid resurfacing using three-dimensional computed tomography of the arthritic glenohumeral joint: the amount of glenoid retroversion that can be corrected. J Shoulder Elb Surg 18:680–688. https://doi.org/10.1016/j.jse.2009.03.019
4. Sabesan V, Callanan M, Ho J, Iannotti JP (2013) Clinical and radiographic outcomes of total shoulder arthroplasty with bone graft for osteoarthritis with severe glenoid bone loss. J Bone Jt Surg Am 95:1290–1296. https://doi.org/10.2106/JBJS.L.00097
5. Walch G, Moraga C, Young A, Castellanos-Rosas J (2012) Results of anatomic nonconstrained prosthesis in primary osteoarthritis with biconcave glenoid. J Shoulder Elb Surg 21:1526–1533. https://doi.org/10.1016/j.jse.2011.11.030
6. Jones RB, Wright TW, Zuckerman JD (2016) Reverse total shoulder arthroplasty with structural bone grafting of large glenoid defects. J Shoulder Elb Surg 25:1425–1432. https://doi.org/10.1016/j.jse.2016.01.016
7. Scalise JJ, Iannotti JP (2008) Bone grafting severe glenoid defects in revision shoulder arthroplasty. Clin Orthop 466:139–145. https://doi.org/10.1007/s11999-007-0065-7
8. Sears BW, Johnston PS, Ramsey ML, Williams GR (2012) Glenoid bone loss in primary total shoulder arthroplasty: evaluation and management. J Am Acad Orthop Surg 20:604–613. https://doi.org/10.5435/JAAOS-20-09-604
9. Wagner E, Houdek MT, Griffith T, Elhassan BT, Sanchez-Sotelo J, Sperling JW, Cofield RH (2015) Glenoid bone-grafting in revision to a reverse total shoulder arthroplasty. J Bone Joint Surg Am 97:1653–1660. https://doi.org/10.2106/JBJS.N.00732
10. Bateman E, Donald SM (2012) Reconstruction of massive uncontained glenoid defects using a combined autograft-allograft construct with reverse shoulder arthroplasty: preliminary results. J Shoulder Elb Surg 21:925–934. https://doi.org/10.1016/j.jse.2011.07.009
11. Iannotti JP, Frangiamore SJ (2012) Fate of large structural allograft for treatment of severe uncontained glenoid bone deficiency. J Shoulder Elb Surg 21:765–771. https://doi.org/10.1016/j.jse.2011.08.069
12. Blumenthal SL, Gill K (1993) Can lumbar spine radiographs accurately determine fusion in postoperative patients? Correlation of routine radiographs with a second surgical look at lumbar fusions. Spine 18:1186–1189
13. Fogel GR, Toohey JS, Neidre A, Brantigan JW (2008) Fusion assessment of posterior lumbar interbody fusion using radiolucent cages: x-ray films and helical computed tomography scans compared with surgical exploration of fusion. Spine J Off J N Am Spine Soc 8:570–577. https://doi.org/10.1016/j.spine.2007.03.013
14. Beheshti M, Mottaghy FM, Paycha F, Behrendt FFF, Van den Wyngaert T, Fogelman I, Strobel K, Celli M, Fanti S, Giammarite F, Krause B (2015) (18)F-NaF PET/CT: EANM procedure guidelines for bone imaging. Eur J Nucl Med Mol Imaging 42:1767–1777. https://doi.org/10.1007/s00259-015-3138-y
15. Cook GJ, Fogelman I (2001) The role of positron emission tomography in skeletal disease. Semin Nucl Med 31:50–61
16. Pumberger M, Prasad V, Druschel C, Disch AC, Brenner W, Schaser K-D (2016) Quantitative in vivo fusion assessment by (18)F-fluoride PET/CT following en bloc spondylectomy. Eur Spine J Off Publ Eur Spine Soc Eur Spinal Deform Soc Eur Sect Cerv Spine Res Soc 25:836–842. https://doi.org/10.1007/s00586-015-4121-9
17. Love C, Din AS, Tomas MB, Kalapparambath TP, Palestro CJ (2003) Radionuclide bone imaging: an illustrative review. Radiogr Rev Publ Radiol Soc N Am Inc 23:341–358. https://doi.org/10.1148/rg.232025103
18. Segall G, Delbeke D, Stabin MG, Even-Sapir E, Fair J, Sajdak R, Smith GT (2010) SNM practice guideline for sodium ^{18}F-fluoride PET/CT bone scans 1.0. J Nucl Med Off Publ Soc Nucl Med 51:1813–1820. https://doi.org/10.2967/jnumed.110.082263
19. Beheshti M, Saboury B, Mehta NN, Torigian DA, Werner T, Mohler E, Wilensky R, Newberg AB, Basu S, Langsteger W, Alavi A (2011) Detection and global quantification of cardiovascular molecular calcification by fluoro18-fluoride positron emission tomography/computed tomography–a novel concept. Hell J Nucl Med 14:114–120
20. Enneking WF, Campanacci DA (2001) Retrieved human allografts : a clinicopathological study. J Bone Joint Surg Am 83-A:971–986
21. Willems WF, Kremer T, Friedrich P, Bishop AT (2014) Surgical revascularization in structural orthotopic bone allograft increases bone remodeling. Clin Orthop 472:2870–2877. https://doi.org/10.1007/s11999-014-3658-y